J|A|C|S
ARTICLES
Published on Web 07/01/2004

Tracing Kinetic Intermediates during Ligand Binding

Tanja Mittag,[†] Brian Schaffhausen,[‡] and Ulrich L. Günther*,[†]

Contribution from the J. W. Goethe University, Frankfurt, Center for Biomolecular Magnetic Resonance, Institute of Biophysical Chemistry, Biocenter N230, Marie-Curie-Str. 9, 60439 Frankfurt, Germany, and Department of Biochemistry, Tufts University, School of Medicine, 136 Harrison Avenue, Boston, Massachusetts 02111

Received October 27, 2003; E-mail: Ulrich.Guenther@em.uni-frankfurt.de

Abstract: Specific protein−ligand interactions are central to biological control. Although structure determination provides important insight into these interactions, it does not address dynamic events that occur during binding. While many biophysical techniques can provide a global view of these dynamics, NMR can be used to derive site-specific dynamics at atomic resolution. Here we show how NMR line shapes can be analyzed to identify long-lived kinetic intermediates for individual amino acids on the reaction pathway for a protein−ligand interaction. Different ligands cause different intermediate states. The lifetimes of these states determine the specificity of binding. This novel approach provides a direct, site-specific visualization of the kinetic mechanism of protein−ligand interactions.

Introduction

Enzymology and structural biology have provided insight into the mechanisms of protein function.[1] However, protein interactions are inevitably influenced or controlled by internal protein dynamics that occur on the micro- to millisecond time scale.[2] The relationship between internal protein dynamics and functions such as catalysis or ligand binding remains poorly characterized. Protein kinetics are often monitored using plasmon resonance and fluorescence methods.[3−5] While plasmon resonance provides an integrated view of binding kinetics with some information about mechanisms, it lacks the resolution to describe protein behavior at the level of individual residues. Fluorescence methods allow a more detailed view at individual sites of interaction and dynamics on a broad time scale for extremely low concentrations of protein, but detailed molecular interpretation of the results is difficult.

NMR spectroscopy provides several possibilities for measuring dynamics on slow time scales. Recently several groups studied the dynamics of protein ligand interactions on a micro- to millisecond time scale by measuring relaxation dispersion using Carr−Purcell−Meiboom−Gill (CPMG) sequences.[6,7] The potential of relaxation dispersion experiments has been explored to study site-specific kinetic events in cyclophilin A where the turnover rate could be assigned to an individual amino acid confirming its role for the catalytic function.[8] Although such measurements allow a quantitative analysis of localized kinetic rates, the underlying kinetic mechanism remains enigmatic.

Line shape analysis of NMR signals can provide a direct view of the mechanism and the kinetic rates of binding events or exchange processes.[9−11] Ligand binding and enzymatic catalysis were previously studied by various NMR methods.[12−15] Line shape analysis of isolated proton signals of the ligand has previously been used to study the catalysis of proline cis/trans isomerization by the isomerase Cyp18.[16] This approach can also be applied to protein signals in two-dimensional (2D) NMR spectra and has been used to study protein folding[17,18] and more recently to investigate protein−ligand interactions.[19−21] By the selection of line shapes from 2D spectra of ^{15}N-labeled proteins, kinetic information was obtained for *individual sites* of the protein.

In this work, we have studied the mechanism of the interactions of the N-terminal src homology 2 domain (N-SH2) of phosphatidylinositide-3-kinase (PI3-K) upon binding of different

[†] J. W. Goethe University.
[‡] Tufts University.

(1) Bruice, T. C.; Benkovic, S. J. *Biochemistry* **2000**, *39*, 6267−74.
(2) Fersht, A. *Structure and Mechanism in Protein Science. A Guide to Enzyme Catalysis and Protein Folding*, 1st ed.; Freeman: New York, 1999.
(3) Engelborghs, Y. *Spectrochim. Acta, Part A* **2001**, *57* (11), 2255−2270.
(4) van Regenmortel, M. H. *Cell. Mol. Life Sci.* **2001**, *58*, 794−800.
(5) Katsamba, P. S.; Park, S.; Laird-Offringa, I. A. *Methods* **2002**, *26* (2), 95−104.
(6) Evenäs, J.; Malmendal, A.; Akke, M. *Structure* **2001**, *9*, 185−195.
(7) Mulder, F. A.; Mittermaier, A.; Hon, B.; Dahlquist, F.; Kay, L. E. *Nat. Struct. Biol.* **2001**, *8*, 932−935.
(8) Eisenmesser, E.; Bosco, D.; Akke, M.; Kern, D. *Science* **2002**, *295*, 1520−1523.
(9) Chan, S.; Reeves, L. *J. Am. Chem. Soc.* **1972**, *95*(3), 673.
(10) Binsch, G. *Dyn. Nucl. Magn. Reson. Spectrosc.* **1975**, 81.
(11) Rao, B. D. *Methods Enzymol.* **1989**, *176*, 279−311.
(12) Lacourciere, K. A.; Stivers, J. T.; Marino, J. P. *Biochemistry* **2000**, *39*, 5630−5641.
(13) Spoerner, M.; Herrmann, C.; Vetter, I. R.; Kalbitzer, H. R.; Wittinghofer, A. *Proc. Natl. Acad. Sci. U.S.A.* **2001**, *98*, 4944−4949.
(14) Tochtrop, G. P.; Richter, K.; Tang, C.; Toner, J. J.; Covey, D. F.; Cistola, D. P. *Proc. Natl. Acad. Sci. U.S.A.* **2002**, *99*, 1847−1852.
(15) Volkman, B. F.; Lipson, D.; Wemmer, D. E.; Kern, D. *Science* **2001**, *291*, 2429−33.
(16) Kern, D.; Kern, G.; Scherer, G.; Fischer, G.; Drakenberg, T. *Biochemistry* **1995**, *34*, 13594−13602.
(17) Balbach, J.; Steegborn, C.; Schindler, T.; Schmid, F. *J. Mol. Biol.* **1999**, *285*, 829−842.
(18) Balbach, J.; Forge, V.; Lau, W. S.; Nuland, N. A.; Brew, K.; Dobson, C. M. *Science* **1996**, *274* (5290), 1161−1163.
(19) Hensmann, M.; Booker, G.; Panayotou, G.; Boyd, J.; Linacre, J.; Waterfield, M.; Campbell, I. *Protein Sci.* **1994**, *3* (7), 1020−30. Jul.
(20) Günther, U. L.; Schaffhausen, B. *J. Biomol. NMR* **2002**, *22*, 201−209.
(21) Günther, U.; Mittag, T.; Schaffhausen, B. *Biochemistry* **2002**, *41*, 11658−11669.

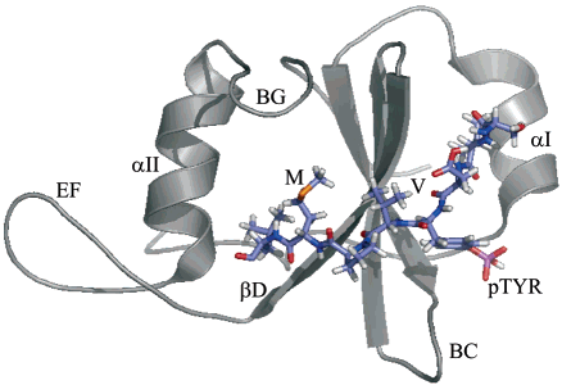

Figure 1. Ribbon diagram of the P395S−PDGFr complex indicating the binding site and the orientation of the bound peptide.[28] The ptyr and the positions ptyr + 1 (V) and ptyr + 3 (M) in the ligand are labeled. The annotation of secondary structural elements follows the convention of Eck et al..[29]

ligands. PI3-K is critical for a broad range of cellular functions including cell growth and survival.[22,23] The structures of many SH2 domains are known.[24] They share common motifs such as a central antiparallel β-sheet flanked by smaller β-sheets and two α-helices. These secondary structural elements are connected by loop regions which are involved in specific ligand interactions. SH2 domains bind phosphotyrosine (ptyr) ligands with ptyr coordinated by two conserved arginines, and they are central to phosphotyrosine signaling pathways.[25]

The N-SH2 used in this work, P395S, is a mutant of the N-SH2 of PI3-K which appeared in random mutagenesis as a mutant with altered specificity compared to the wild-type N-SH2.[26] For this mutant, specificity for the residue immediately C-terminal to the phosphotyrosine (+1) changed from M, V, I, E for wild-type to V, and the specificity for M at +3 seen for wild-type is lost in the mutant.[27] As a result, this N-SH2 mutant retains high affinity for the platelet-derived growth factor receptor (PDGFr, PI3-K N-SH2 binding sequence: pY**V**PM), while having a reduced affinity for the polyomavirus middle T oncoprotein (MT, PI3-K N-SH2 binding sequence: pY**M**PM). Although the point mutation occurs on a surface loop involved in coordination of the +3 residue, there are differences in structure extending beyond the site of the mutation.[28] The binding region of the P395S N-SH2 domain for the peptide derived from PDGFr is depicted in Figure 1. Large parts of the protein are involved in ligand complexion. The ptyr binding pocket is formed by residues in α-helix I, the central β-sheet and the BC loop. The peptide stretches over the β-sheet, where the BG loop is involved in many contacts to the peptide.

The mechanism of the interactions of the P395S N-SH2 domain with phosphotyrosine-containing ligands has been studied using NMR line shape analysis of two-dimensional ^{15}N heteronuclear single quantum coherence (HSQC) spectra. We visualize for the first time *intermediates in ligand binding* for individual amino acids. For different peptide ligands, the lifetime and position of intermediates on the reaction pathway determine the specificity of the interaction. The proposed line shape analysis should be broadly applicable to study protein−ligand interactions of moderately sized proteins.

Results and Discussion

In this work, line shape analysis of NMR signals has been used to probe the kinetic behavior of the N-SH2 domain of PI3-kinase upon binding of different phosphotyrosine-containing ligands. Titrations of the P395S N-SH2 mutant for two peptides derived from PDGFr and MT were compared to each other and to titrations of the wild-type N-SH2 domain with the same peptides. The resonances in HSQC spectra of the wild-type N-SH2 recorded for increasing amounts of MT peptide are typical for a simple one-step binding event (P + L ⇌ PL). ^{15}N cross sections of the signal of S339 (αA1) in the wild-type N-SH2 are depicted in Figure 2a (lines with triangles), where the signal of the free protein is shown in blue. For increasing amounts of peptide, the color changes from blue to red, where red represents the fully complexed protein. Simulations of the line shapes (shown as solid lines) support a one-step binding mechanism.[20,21]

For P395S, the titration with MT peptide (Figure 2b) showed novel behavior that cannot be explained by one-step binding. As increasing amounts of peptide are added to the free P395S N-SH2 domain (color coding as in Figure 2a), the chemical shifts of the intermediate lines change successively as expected for a binding event that is fast on the NMR time scale. The signals seem to "bunch" between 90 and 100 Hz, and in the eighth step of the titration (at a protein/peptide concentration ratio of 1:0.89), the signal has a large shoulder indicated by an arrow in Figure 2b. This additional complexity in NMR line shapes requires at least one intermediate on the binding pathway that will be denoted PL*. Shifts of the starting signal (blue) are caused by a fast off-rate that averages the signal between the free N-SH2 (P) and the intermediate (PL*) which is generated from the free protein upon association with the ligand (L). The position of the signal between P and PL* reflects changing populations of the two states. The signal shoulder (arrow) indicates slow exchange on an NMR time scale between the intermediate and the final complex (PL, red). These lines were simulated employing the following mechanism:

$$\mathrm{P} + \mathrm{L} \underset{k_{\mathrm{off},1}}{\overset{k_{\mathrm{on},1}}{\rightleftharpoons}} \mathrm{PL}^* \underset{k_{\mathrm{off},2}}{\overset{k_{\mathrm{on},2}}{\rightleftharpoons}} \mathrm{PL} \qquad (1)$$

However, simulations showed that the conversion from PL* to the final product PL also depends on the concentration of the ligand. To account for the 1:1 stoichiometry of the interaction, a more complex mechanism, where L is intermediately released from PL*, must be assumed. The simplest way to summarize this reaction scheme yields a mechanism of the type:

$$\begin{array}{ccc} \mathrm{P} + \mathrm{L} & \underset{k_{\mathrm{off},1}}{\overset{k_{\mathrm{on},1}}{\rightleftharpoons}} & \mathrm{PL}^* \\ & & \Downarrow \\ & & \mathrm{P}^* + \mathrm{L} \underset{k_{\mathrm{off},2}}{\overset{k_{\mathrm{on},2}}{\rightleftharpoons}} \mathrm{PL} \end{array} \qquad (1a)$$

(22) Fantl, W. J.; Escobedo, J. A.; Martin, G. A.; Turck, C. W.; del Rosario, M.; McCormick, F.; Williams, L. T. *Cell* **1992**, *69* (3), 413−423.
(23) Valius, M.; Bazenet, C.; Kazlauskas, A. *Mol. Cell. Biol.* **1993**, *13*, 133−143.
(24) Kuriyan, J.; Cowburn, D. *Annu. Rev. Biophys. Biomol. Struct.* **1997**, *26*, 259−288.
(25) Cantley, L. C. *Science* **2002**, *296* (5573), 1655−57.
(26) Yoakim, M.; Hou, W.; Liu, Y.; Carpenter, C. L.; Kapeller, R.; Schaffhausen, B. S. *J. Virol.* **1992**, *66* (9), 5485−5491.
(27) Songyang, Z.; Shoelson, S.; Chaudhuri, M.; Gish, G.; Pawson, T.; Haser, W.; King, F.; Roberts, T.; Ratnofsky, S. *Cell* **1993**, *72* (5), 767−778.
(28) Günther, U.; Weyrauch, B.; Zhang, X.; Schaffhausen, B. *Biochemistry* **2003**, *42*, 11120−11127.

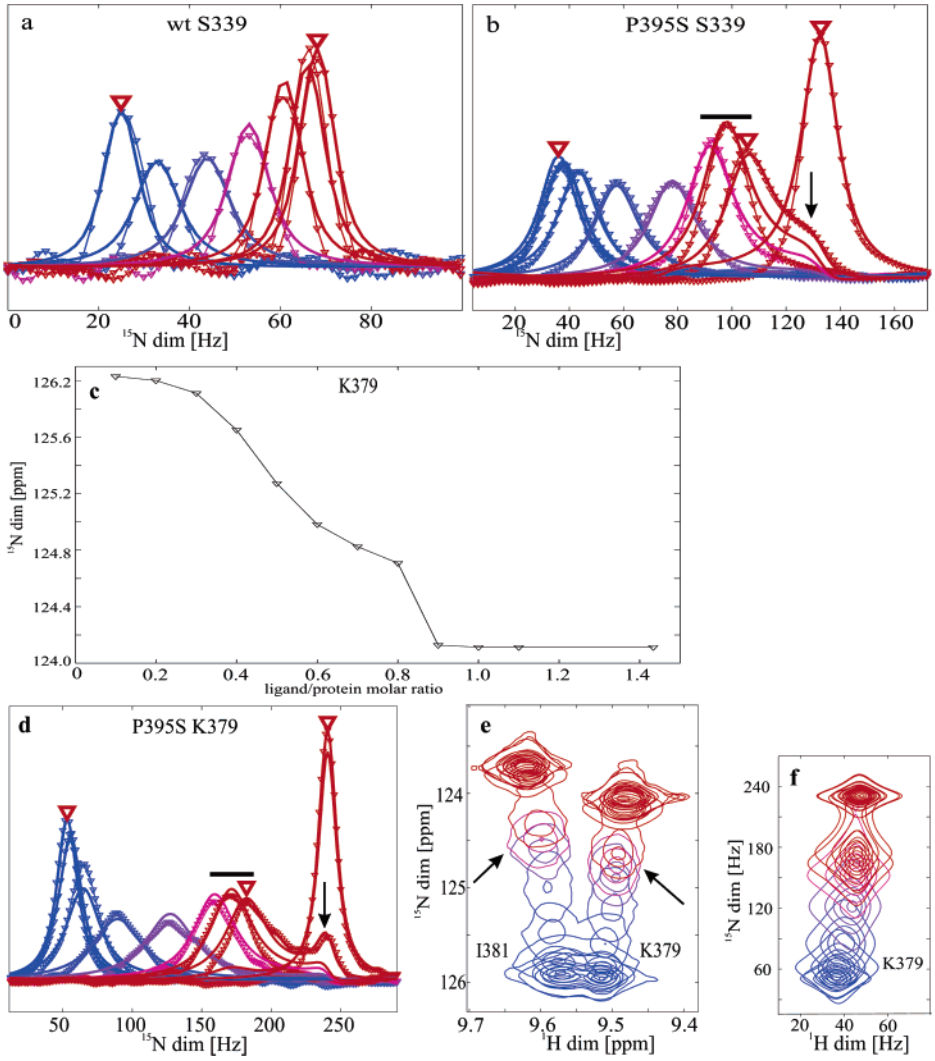

Figure 2. Comparison of line shapes from HSQC spectra of the wild-type N-SH2 with P395S. (a) ^{15}N cross section from two-dimensional HSQC spectra of S339 for subsequent steps of a titration of the wild-type N-SH2 with MT peptide (lines with ∇ from blue to red) and line shapes simulated (solid lines) for a one-step binding model (P + L ⇌ PL). In the same titration for the P395S mutant, "bunching" of signals in ^{15}N slices of (b) S339 and (d) K379 is marked with a solid bar. The simulations are carried out according to the sequential mechanism 1. (c) A binding curve for the ^{15}N dimension of K379 shows intermediate formation at a molar fraction of the ligand of 0.7. (e) Experimental two-dimensional cross peaks of K379 and I381 for sequential steps of a titration show bunching of signals marked with arrows. (f) Simulated two-dimensional signal. Quantitative estimates for the off-rates. P395S S339: $k_{off,1} > 5000\ s^{-1}$, $k_{off,2} \approx 18[-8 + 8]\ s^{-1}$, $K = k_{on,2}/k_{off,2} \approx 2$. K379: $k_{off,1} \approx 2120[-520 + 820]\ s^{-1}$, $k_{off,2} \approx 26[-10 + 11]\ s^{-1}$, $K = k_{on,2}/k_{off,2} \approx 50$.

The intermediate step in brackets involving a long-lived P* is not observed in line shapes. Off-rates obtained from NMR line shape simulations represent the reciprocal lifetimes ($\tau = 1/k_{off}$) of PL* and PL.

This type of intermediate formation is even more pronounced for residues at the phosphotyrosine + 1 binding site on the central β-sheet such as for residue K379 for which two distinct signals are observed in the eighth titration step (arrow in Figure 2d). Simulations using mechanism 1 provide good fits for both ^{15}N and ^{1}H cross sections of the signal, and most importantly, the similarity of experimental (Figure 2e) and simulated (Figure 2f) two-dimensional signals validate the model. Quantitative estimates for the off-rates are presented in the caption of Figure 2. In both cases, the off-rate of the second step was more than 1 order of magnitude smaller than the off-rate of the first step.

Intermediate formation upon binding of MT peptide was observed throughout the protein for 24 out of 61 titrating residues labeled magenta on the ribbon diagram in Figure 3a. Residues showing similar kinetics were located in regions of the protein involved in the ligand interaction including residues in the αB-helix, the EF loop, the central β-sheet, and the ptyr binding pocket (Figure 1). The off-rate of the first step was fast ($500\ s^{-1} < k_{off,1} < 6000\ s^{-1}$), while the second step had a low off-rate ($12\ s^{-1} < k_{off,1} < 35\ s^{-1}$) and a small equilibrium constant ($2 < K < 50$) favoring the final product PL. The observed variation on off-rates at different sites of the protein represents differences in lifetimes of a particular state in the ligand interaction for individual amino acids.

The large amount of residues which show a two-step kinetic mechanism covers the entire binding region of the binding pocket. Transfer of kinetic events over large parts of the protein is consistent with previous observations which showed that alterations of the peptide in the ptyr + 3 position affects the chemical shifts of the protein resonances in the ptyr pocket. The second binding step must be attributed to a rearrangement which follows ligand binding. The possibility of unspecific interactions at high ligand concentrations suggested by a reviewer can be ruled out because the interaction would be too

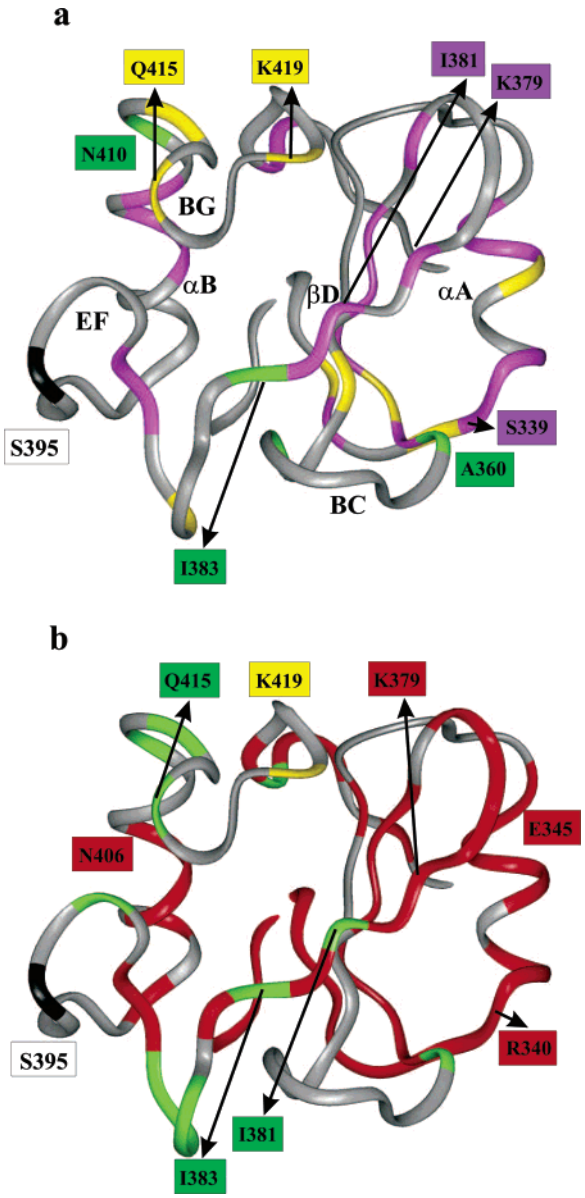

Figure 3. Line shape patterns of residues of the P395S mutant of the p85 N-SH2 domain for titrations with (a) MT peptide and (b) PDGFr peptide mapped onto the structure of the free N-SH2 domain.[30] Residues are depicted in different colors according to observed line shape patterns (magenta, model 1a with slow exchange in second step; yellow, model 1a with fast exchange in second step; red, model 2; green, complex line shapes). Key residues mentioned in the text are labeled separately. The mutation site, S395, is shown in black.

weak to cause slow exchange in spectra as observed for many residues (e.g., K379 in Figure 2d). In addition, unspecific binding should be observed after a stoichiometric amount of ligand has been bound to the protein, and unspecific interactions should also be observed for the other ligand and for the wild-type protein.

Ten residues (labeled yellow in Figure 3a) showed different types of line shapes in the titration with MT peptide. The resonances of Q415 represent one example (Figure 4). The concentration of the intermediate is consistently low, and lines shift before and after intermediate formation. As in the first case, it is the interaction with ligand that establishes a binding intermediate. Simulation of two-dimensional line shapes showed that the spectra can be explained by the same sequential model

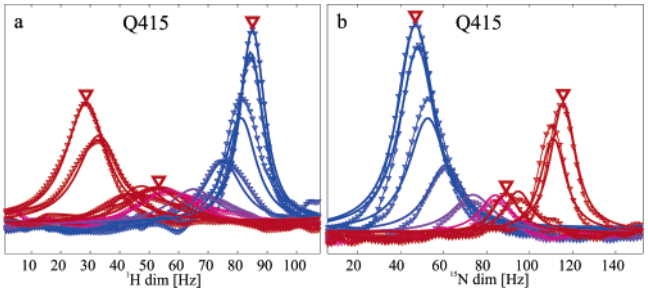

Figure 4. Line shapes from HSQC spectra of the P395S N-SH2 domain in a titration with MT peptide. Cross sections of the (a) ^{1}H and (b) ^{15}N dimension of signals of Q415 for steps of the titration from blue to red. Experimental lines are shown with ∇, and simulated signals are shown as solid lines. The simulation of the two-dimensional signal for the sequential reaction 1 yielded the off-rates $k_{off,1} \approx 800\ s^{-1}$ and $k_{off,2} \approx 600\ s^{-1}$. The concentration of the intermediate PL* is relatively low. The resonance frequencies of P, PL*, and PL are marked by red triangles.

(eq 1a). However, here the off-rate of the second binding step is much higher causing fast-exchange line shapes for both steps of the reaction ($k_{off,1}$ 800 s^{-1} and $k_{off,2} \approx 600\ s^{-1}$). Essentially, the second binding step requires rearrangements brought about by the first step in a quasi-allosteric fashion. Most of the residues showing this behavior are either in the BG loop or involved in phosphotyrosine coordination including R358, one of the arginines coordinating the ptyr phosphate.

Interaction of the P395S N-SH2 domain with the PDGFr peptide is characterized by a higher affinity and shows very different kinetic properties. Out of 68 titrating residues, 38 show line shapes reflecting a simple one-step binding reaction starting *not* from the signal of the free N-SH2 but rather starting from the second spectrum of the titration series. Line shapes for N406 (Figure 5a and b) show an example of this behavior. The *first step* causes small changes in both dimensions of the spectrum. In the ^{1}H dimension, the signal in the first spectrum is shifted to lower field with the first addition of ligand (Figure 5a). There is also an increase in intensity. In the ^{15}N dimension of N406, we observe a significantly increased intensity and reduced width of the line with almost no shift in the first titration step in contrast to the following ones. Since only a small volume of 2 μL of peptide dissolved at the same pH and salt concentrations as the protein was added, these effects cannot be caused by dilution, change of salt concentrations, or change in pH.

Instead this behavior of signals requires an intermediate P* which is formed by an initial interaction with ligand L. The subsequent titration starts from the intermediate species P* (labeled with a red ∇ in Figure 5b and c) and shows typical characteristics of a two-site binding between P* and PL. This can be described by a simple mechanism of the form

$$P \underset{k_{off,1}}{\overset{[L],k_{on,1}}{\rightleftharpoons}} P^* + L \underset{k_{off,2}}{\overset{k_{on,2}}{\rightleftharpoons}} PL \qquad (2)$$

The line shapes for PDGFr can be well described employing this mechanism. While the first step of this reaction does not necessarily involve specific interactions with the ligand, an encounter with ligand may produce a conformational change or stabilize a conformer of a preexisting equilibrium. This event is necessary for productive binding. The actual role of the ligand in the formation of P* cannot be elucidated from this NMR analysis, but less than 0.1 equiv of PDGFr peptide is required for the conversion while the overall stoichiometry of the

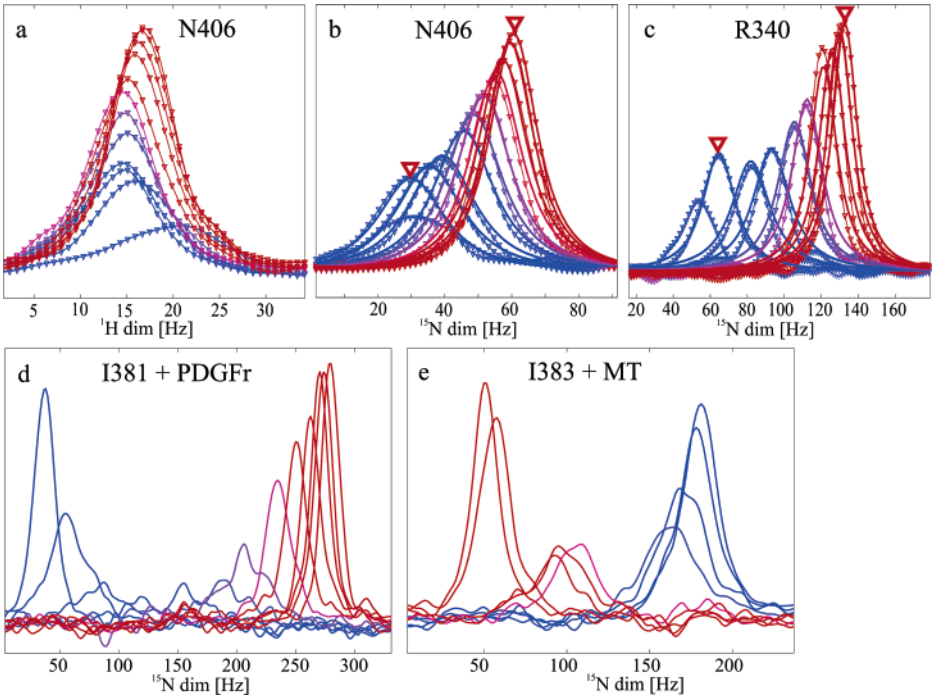

Figure 5. Line shapes from ^{1}H−^{15}N HSQC spectra of the P395S N-SH2 domain in titrations with MT and PDGFr peptide. (a−c) P395S N-SH2 interaction with a PDGFr peptide shows rearrangement prior to two-site binding. (a) ^{1}H and (b) ^{15}N cross sections of N406 in a titration of the P395S N-SH2 with PDGFr peptide. The line shapes can be simulated with a one-step reaction scheme (P + L ⇌ PL) and an off-rate $k_{off} \approx 1000$ s^{-1} if two-site exchange starts from the second spectrum. (c) In the ^{15}N dimension of R340, the simulation starting from the second spectrum (labeled with a red 5) yields an off-rate of $k_{off,2} \approx 1500$ s^{-1}. Experimental lines are shown with ∇, and simulated signals are shown as solid lines (—) from blue to red for subsequent steps of the titration. (d−e) Complex line shapes indicate the formation of several conformers on the reaction pathway. (d) The ^{15}N cross sections of I381 for subsequent steps of the titration of the P395S N-SH2 with PDGFr peptide exhibit the formation of signal shoulders after addition of ligand. (e) The ^{15}N cross sections of I383 in a titration with MT peptide exhibit several shoulders in intermediate titration steps. Additionally the overall shape of the lines indicate the sequential mechanism 1a.

interaction remains 1:1. In this instance, simulations reveal that P* has a long lifetime and the reverse reaction back to P is unlikely. The off-rate of the second step $k_{off,2}$ is relatively high, as required for fast exchange, and ranges between 200 s^{-1} and 2000 s^{-1}.

Residues showing this type of behavior (labeled red on the ribbon diagram in Figure 3b) were typically located in the α-helices and β-sheets including the arginines R340 (Figure 5c) and R358 which coordinate the phosphotyrosine phosphate. For R340, a distinct first step is observed followed by binding with a relatively high off-rate (1500 s^{-1}) typical for an interaction with relatively low affinity ($K_D = k_{off}/k_{on}$). Low off-rates of 320 s^{-1} and 270 s^{-1} indicative of a higher affinity interaction were observed for E345 and K346 in the αA-helix.

An increased intensity after adding PDGFr peptide was observed for many but not for all residues of P395S. The same effect was also observed for the wt N-SH2. The lower intensity of some signals in the free N-SH2 can be attributed to exchange at different time scales. This could be supported by the observation of micro- to millisecond exchange in some positions of the protein[31] whereas H/D exchange rates did not correlate well with decreased signal intensities. The possibility of concentration-dependent aggregation in the free protein suggested by a reviewer can be ruled out based on line widths of the P395S N-SH2 recorded for different concentrations. The solution structure of the P395S N-SH2 domain reveals a perturbance of the usual tertiary structure in the small β-sheet and the EF loop, the region around the mutation site.[28] The normal fold is partially restored upon ligation. Differences in signal intensities can therefore be attributed to altered exchange properties in the stabilized complex compared to a flexible free protein undergoing conformational exchange.

Even more complex kinetic behavior is observed for some residues. Examples are depicted in Figure 5d and e. Here signals show multiple shoulders corresponding to different long-lived conformers created upon an encounter with ligand. Toward the end of the titration the signal is refocused. Although line shapes are too complex to be simulated, a plausible mechanism is ligand-induced formation of intermediates which can then bind ligand in a parallel reaction scheme. This is shown for the example of three parallel reactions:

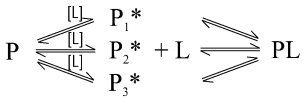

(3)

Each of these encounters could be of the same type as described by eq 1a or 2.

This kind of line shape was observed for only 4 residues in the MT peptide titration (A360, A366, I383, and N410 shown in green in Figure 3a) and for 10 residues in the titration with PDGFr peptide (A360, G366, I381, I383, S393, N410, S412, Q415, K419, and L424 labeled in green in Figure 3b). Interestingly, I381 showed smooth lines for the titration with

(29) Eck, M. J.; Shoelson, S. E.; Harrison, S. C. *Nature* **1993**, *362*, 87−91.
(30) Weber, T.; Schaffhausen, B.; Liu, Y.; Günther, U. *Biochemistry* **2000**, *39*, 15860−15869.
(31) Mittag, T.; Schaffhausen, B.; Günther, U. L. *Biochemistry* **2003**, *42*, 11128−11136.

MT peptide, similar to those of K379 in Figure 2d and typical for mechanism 1a, but it exhibited complex line shapes in the titration with PDGFr peptide. Signals of A360 and I383 in the titration with MT peptide exhibit the overall shape of lines which can be simulated using mechanism 1. However, the signals of intermediate spectra show shoulders. The signal of A360 also shows complex lines in titrations of the wild-type protein.[21] For this residue, this behavior may simply reflect a transfer of conformational flexibility from the BC loop. The same effect is also observed in residues in the flexible BG loop which show complex lines (S412, Q415) and reduced intensity (R409, A414).

The results presented here demonstrate the potential of NMR line shape analysis to detect differences in binding mechanisms for different ligands toward the same protein target. There are two major advantages to this approach. One is that, in comparison to methods such as plasmon resonance or fluorescence spectroscopy, a residue specific picture of the binding process is obtained. Almost half of the residues of the N-SH2 could be analyzed individually. Another particular value of this approach is that kinetic rates can be determined by studying steady-state line shapes at different ligand concentrations, although measuring times in NMR spectroscopy are much longer than those lifetimes. In addition, kinetic models both explain the observed spectra and provide quantitative estimations of reaction rates.

The aim of this work was to understand changes in affinity for two different ligands, PDGFr and MT, for the N-terminal SH2 domain of PI3-kinase. Modeling of the two-dimensional NMR signals has provided key insights into the mechanism of the interaction. The high affinity PDGFr peptide ligand induces a stable intermediate N-SH2 on the reaction path to binding. The lower affinity MT peptide generates a different, less stable intermediate. No conformational heterogeneity could be detected in either the free N-SH2 or the final complex.

Line shapes in titrations with the higher affinity PDGFr ligand showed two-site binding after initial rearrangement of the protein or stabilization of a conformer (eq 2). The intermediate formed has a relatively long lifetime (that is a small $k_{off,1}$). For this reason, it must be formed with small concentrations of ligand and there is no direct competition between the two steps of the binding reaction. The intermediate for PDGFr is probably structurally similar to the starting protein because there are only small chemical shift changes between the first spectra. A kinetic hindrance of the conversion from P to the thermodynamically more stable P* must be reduced by addition of ligand.

Line shapes in titrations with the lower affinity MT peptide show the formation of an intermediate with a relatively fast off-rate ($k_{off,1}$), a clear indication that the intermediate lacks stability. Formation of the final product requires a second binding event (see eq 1a). Consequently the first step is an unproductive attempt of a transition to a form which can bind the ligand with high affinity. Since the stoichiometry is 1:1 for the overall interaction, the ligand must be "recycled" for the second binding step. For the MT peptide, a much higher energy barrier must be overcome and the intermediate is not kinetically stabilized. Large chemical shift changes (see intermediates marked in Figure 2) between the intermediate and the free protein suggest significant structural changes.

Additional complexity seen in the line shapes of some residues in the PDGFr titration sheds light on the structural basis for the observed rearrangements. Residues in βD (I381 and I383) and BG (N410, S412, Q415, and K419) show shoulders in line shapes that cannot occur for two-site binding and that require at least one intermediate each. These signal components reflect the formation of kinetically stable conformers by small amounts of ligand. This must be a concerted rearrangement involving some part of the central β-sheet and the BG loop. This view is supported by the similarity in complexity of line shapes of residues marked green in Figure 3b. Interestingly, these effects can be induced by V but not M in the ptyr + 1 position of the ligand. Since formation of intermediates is also seen in these regions in wild-type, they appear to be important for effective binding. The geometry and mobility of the V side chain must be more favorable for inducing these changes.

Conclusions

The mechanism derived here from NMR line shapes of protein signals in ligand titrations describes a novel view of protein−ligand interaction. Despite ongoing efforts to characterize intermediates in protein folding (see ref 32 and references therein), site-specific rearrangements of proteins during ligand binding have only recently been analyzed.[21]

These results demonstrate that specificity in ligand binding is controlled kinetically for the interaction of the N-SH2 mutant P395S with different phosphopeptides. The initial interaction with the higher affinity PDGFr peptide probably induces the formation of an intermediate state which is able to bind ligand with high affinity, whereas an intermediate late on the reaction pathway for binding of MT peptide represents a kinetic hindrance for the conversion to the final product. From initial results of titrations with other proteins, we expect that similar kinetic mechanisms will prove to be common.

Basic limitations of the method are the line width of the resonances in HSQC spectra and chemical shift degeneracy of signals. The kinetic rates must be in the window of fast to intermediate exchange on the NMR time scale. This window can be expanded by the choice of the magnetic field strength. Although the structures of the intermediates are usually not accessible, the visualization of intermediates in spectra provides substantial new information to understand protein−ligand interactions. The existence of these intermediate states may have important practical implications. Sites involved in, or required for, the dynamic changes in ligand binding may represent new targets in the development of therapeutics.

Materials and Methods

Sample Preparation and NMR Spectroscopy. The mutant N-SH2 pGEX3X-GST-N-SH2 construct (amino acids 321 to 434) and the NMR samples were expressed and purified as described previously.[33,34] ^{15}N-labeled SH2 was prepared using minimal medium with $^{15}NH_4Cl$ as a sole source of ^{15}N (Cambridge Isotope Laboratories). Factor Xa (Haematologic Technologies) was used to cleave the N-SH2 from the fusion protein. The N-SH2 was further purified by gel chromatography (Superdex 75) in 0.1 M KCl solution with 0.02% of NaN_3, pH 6.8. The purity of proteins was judged by gel chromatography and the fact that ^{1}H−^{15}N HSQC spectra showed a unique set of assigned signals. Phosphopeptides were synthesized and HPLC purified by the Tufts

(32) Myers, J.; Oas, T. *Annu. Rev. Biochem.* **2002**, *71*, 783−815.
(33) Yoakim, M.; Hou, W.; Songyang, Z.; Liu, Y.; Cantley, L.; Schaffhausen, B. *Mol. Cell. Biol.* **1994**, *14* (9), 5929−5938.
(34) Günther, U.; Liu, Y.; Sanford, D.; Bachovchin, W.; Schaffhausen, B. *Biochemistry* **1996**, *35* (48), 15570−15581.

Protein Chemistry Facility. Their purity was confirmed by NMR spectra and ESI or MALDI mass spectra. Peptides used were EEEpYMPME-NH_2 derived from the known PI3-K binding site of polyomavirus middle T sequence around the tyrosine phosphorylation site at residue 315 (MT peptide) and SVDpYVPML-NH_2 derived from the PDGF receptor sequence at the 751 binding site (PDGFr peptide). The freeze-dried peptides were dissolved in 0.1 M KCl solutions, and the pH was carefully adjusted to 6.8. Concentrations of protein and peptide were measured by UV absorption at 279 nm (using extinction coefficients of 610 L cm^{-1} mol^{-1} for ptyr in peptides[35,36] and an extinction coefficient of 20 735 L cm^{-1} mol^{-1} for the N-SH2). The P395S N-SH2 samples had concentrations of 1.0 mM in the titration with MT peptide and 0.5 mM in the case of the titration with the PDGFr peptide. Peptide concentrations were 41 mM for the MT peptide and 12.5 mM for the PDGFr peptide. The typical volume of peptide solution added in one titration step was 1.5 or 2 μL in a total volume of 500 μL. After each addition of peptide, the homogeneity of the static magnetic field was readjusted and the tuning of the probe circuit was checked. The titration was continued until no chemical shift changes were observed in the HSQC spectra, resulting in 9 (MT peptide) and 11 (PDGFr peptide) titration steps. A last addition of one portion of peptide solution confirmed the end of the titration, resulting in a small excess of peptide. $^1H-^{15}N$ HSQC spectra were recorded on a BRUKER DMX 500 spectrometer at 303 K with 16 scans and 2048 $\times$ 700 points to obtain sufficient spectral resolution for line shape analysis in both dimensions.

Spectra were processed employing qsine window functions, and line shapes were extracted from two-dimensional spectra using NMRLab[37] ensuring the careful selection of the slices of the peak maxima. To avoid errors by not selecting the maximum of the signal, sufficient zero filling was used in the line shape simulation process and both dimensions were graphically represented by the simulation program to avoid such errors.

Line Shape Analysis. The details of line shape simulation were reported by Guenther et al.,[20] using the software NMRKIN which calculates the *time domain signal* for sections of HSQC spectra for different kinetic mechanisms assuming steady-state line shapes as described by the equations of Gutowsky and later McConnell.[38,39] Positions of signals, line widths, populations, and kinetic rates were adjusted iteratively to achieve consistency with experimental data. For the calculations, we assume steady-state conditions wherefore exchange does not have to be simulated during the INEPT transfers. Unlike in the original NMRKIN software, the complete two-dimensional signal is calculated. This is necessary when intermediates appear in cross-peaks of two-dimensional signals. Calculating line shapes in the time domain with subsequent Fourier transformation allowed the use of apodization functions identical to those used for the experimental data. The error of the calculated rates depends on their absolute values.[21] The kinetic window for which kinetic parameters can be determined precisely from line shapes depends on the chemical shift differences of the species involved in the reaction. The simultaneous simulation of both spectral dimensions improves the quality of the parameter values remarkably because it reduces the degrees of freedom. As reported previously,[21] the experimental errors of rates are only insignificantly larger than theoretical errors. For off-rate $k_{off,1}$ in the sequential model for K379 in the MT-titration, a theoretical lower error of -520 Hz and an upper error of $+820$ Hz is obtained, whereas the experimental error is only 2% and 4.3% larger for the lower and upper limit, respectively. We obtain $k_{off,1} = 2120[-530 + 855]$ s^{-1}. For $k_{off,2} = 26$ s^{-1}, the theoretical confidence interval is 17 to 36 s^{-1}, and the experimental confidence interval is 16 to 37 s^{-1}.

Acknowledgment. This work was supported by the European Large Scale Facility Frankfurt and by grants from the NIH to B.S.

Supporting Information Available: Populations of different states as used in the line shape simulations and series of HSQC spectra of the P395S N-SH2 domain in titrations with MT peptide and PDGFr peptide.

JA0392519

(35) Zhang, Z.; Maclean, D.; Thieme-Sefler, A.; Roeske, R.; Dixon, J. *Anal. Biochem.* **1993**, *211*, 7−15.
(36) Zhao, Z.; Zander, N.; Malencik, D.; Anderson, S.; Fischer, E. *Anal. Biochem.* **1992**, *202*, 361−366.
(37) Günther, U.; Ludwig, C.; Rüterjans, H. *J. Magn. Reson.* **2000**, *145* (2), 201−208.
(38) Gutowsky, H.; McCall, D.; Slichter, C. *J. Chem. Phys.* **1953**, *21* (2), 279−292.
(39) McConnell, H. M. *J. Chem. Phys.* **1958**, *28*, 430−431.